Conformational changes in cubic insulin crystals in the pH range 7–11

Olga Gursky, John Badger, Youli Li, and Donald L. D. Caspar
Rosenstiel Basic Medical Sciences Research Center, Brandeis University, Waltham, Massachusetts 02254-9110 USA

ABSTRACT To determine the effect of variations in the charge distribution on the conformation of a protein molecule, we have solved the structures of bovine cubic insulin over a pH range from 7 to 11 in 0.1 M and 1 M sodium salt solutions. The x-ray data were collected beyond 2-Å resolution and the R factors for the refined models ranged from 0.16 to 0.20. Whereas the positions of most protein and well-ordered solvent atoms are conserved, about 30% of residues alter their predominant conformation as the pH is changed. Conformational switching of A5 Gln and B10 His correlates with the pH dependence of monovalent cation binding to insulin in cubic crystals. Shifts in the relative positions of the A chain NH_2-terminal and B chain COOH-terminal groups are probably due to titration of the A1 α-amino group. Two alternative positions of B25 Phe and A21 Asn observed in cubic insulin at pH 11 are similar to those found in two independent molecules of the 2Zn insulin dimer at pH 6.4. The conformational changes of the insulin amino acids appear to be only loosely coupled at distant protein sites. Shifts in the equilibrium between distinct conformational substates as the charge distribution on the protein is altered are analogous to the electrostatically triggered movements that occur in many functional protein reactions.

INTRODUCTION

Cubic insulin crystals (space group $I2_13$, unit cell parameter 78.9 Å) (Dodson et al., 1978; Badger et al., 1991) contain a solvent volume of 65% (Badger and Caspar, 1991) and are stable in low ionic strength monovalent cation salt solutions over a wide range of pH (Gursky et al., 1992). Thus, they provide a particularly favorable system for crystallographic studies of pH-dependent structural changes in proteins under nearly physiological conditions. To investigate the role of specific electrostatic interactions in protein conformational switching, we have determined high resolution structures of the cubic insulin crystals at pH values varying from 7 to 11. Over this pH range the net negative charge on the protein is increased from about −2 to about −6 as specific amino acids are titrated. In this paper we describe the structural changes in cubic insulin crystals that result as some of the amino acid groups are titrated, analyze the effects of salt concentration on these changes, and correlate these effects with changes in the occupancies of the cations that neutralize the charge on the protein.

X-ray crystallographic studies performed over wide ranges of pH with plastocyanin (Guss et al., 1986), γ-chymotrypsin (Dixon et al., 1991), and azurin (Nar et al., 1991) revealed only small conformational transitions localized near some of the titratable histidine groups. The absence of more significant structural changes in response to amino acid titrations in these crystals might be due to extensive shielding of charged groups at the high ionic strengths that were used in all these experiments. It would be expected that our experiments on cubic insulin crystals, in which 55% of the protein surface is in contact with the solvent of nearly physiological ionic strength (Badger and Caspar, 1991), would show greater sensitivity of the protein conformations in response to changes in pH.

Address correspondence to Dr. Olga Gursky, Rosenstiel Basic Medical Sciences Research Center, Brandeis University, Waltham, MA 02254-9110.

MATERIALS AND METHODS

Cubic zinc-free crystals of bovine insulin were grown from 0.25 M sodium phosphate solution at pH 9.2 (Dodson et al., 1978; Gursky et al., 1992) and equilibrated by dialysis against sodium salt solutions that varied in pH from 7 to 11. At pH < 7 the crystals gradually turned brown and the lattice order was disrupted, and in more alkaline solutions the crystals dissolved. The presence of sodium or other small monovalent cations at 0.1 M concentration was essential for crystal stability in the pH range from 7 to 10 (Gursky et al., 1992), while at pH 11 higher salt concentration was required to prevent crystals from dissolving. Experiments with bovine insulin crystals were carried out at pH 7–10 with both 0.1 and 1.0 M sodium concentrations, and at pH 11 with 1.0 M sodium concentration. Mixtures of sodium acetate and sodium carbonate were used to adjust the pH in the range from 7 to 10 together with 0.02–0.04 M Tris/HCl buffer. Experiments were also made with crystals grown from sodium or potassium phosphate solutions and equilibrated against solutions containing 0.1 M in potassium at pH 7–10.

X-ray diffraction data extending to beyond 2-Å resolution were collected at room temperature from single cubic bovine insulin crystals at pH 7, 8, 9, and 10 in 0.1 M Na or K, and at pH 7, 9, and 11 in 1.0 M Na using the Brandeis TV Area Detector (Kalata, 1985; Kalata et al., 1990) with an Elliott rotating anode generator and Cu K_α radiation. Crystal slippage during the data collection was prevented by coating the crystals in the capillaries with a Formvar film by evaporation from dichloroethane solution (Rayment et al., 1977), which resulted in dichloroethane binding to the insulin molecular dimer (see below). Data were collected from single crystals in 0.1° frames (90-s exposure time per frame) over a rotation range of 90°, and processed using the MADNES program (Pflugrath and Messerschmidt, 1987) modified for the Brandeis Area Detector. The peak intensities were obtained by three-dimensional profile fitting with subsequent corrections for radiation damage and absorption (Kabsch, 1988). A summary of the data collected from the bovine insulin crystals under various solvent conditions is given in Table 1.

The structure of cubic bovine insulin at pH 9 in 0.1 M Na was refined using the previously solved structure of cubic porcine insulin (Badger et al., 1991) as an initial model. The structure of cubic bovine insulin at pH 9 in 0.1 M sodium was then used as the starting point for solving the structures at other solvent conditions. Atomic coordinates and temperature factors were refined by restrained least-squares minimization (Hendrickson, 1985) using the FFT algorithm (Agarwal, 1978), and

0006-3495/92/11/1210/11 $2.00

TABLE 1 **Summary of the x-ray data and processing statistics**

Solvent cation concentration	pH	Resolution limit	Total number of reflections	Number of unique reflections	Completeness of data	R_{merge}‡
M		Å			%	%
0.1 Na	7	2.0	21,745	5,431	100	9.5
	8	1.9	24,280	5,277	85	5.6
	9	1.9	21,890	5,760	93	5.3
	10	1.9	24,331	6,281	100	9.5
1.0 Na	7	1.9	12,262	4,522	60	6.2
	9	2.0	26,222	4,800	89	5.2
	11	1.9	21,417	5,588	90	6.9
0.1 K	8	1.9	17,496	5,926	86	7.2
	9	2.6	9,414	2,039	82	5.9
	9*	2.6	9,617	2,004	81	6.1
	10	1.9	24,056	5,715	93	8.7

Resolution, number of reflections collected, completeness of data in the range between 10 Å and the highest resolution available, and merging R factor for the symmetry-related reflections are shown. Data were collected from single crystals of cubic bovine insulin grown from sodium salt solution and equilibrated against sodium or potassium salt solutions at different pH and salt concentrations.

* Data were collected from crystals grown from potassium salt solution.

† R_{merge} was calculated based on intensities of all equivalent reflections (including symmetry-related reflections and reflections in different runs on the same crystal that were used to scale the runs). R_{merge} values for different resolution shells range from ~3.5% at a resolution below 4.5 Å to ~15% at 2 Å resolution. The completeness of the data in the outermost resolution shells (<2.1 Å) is typically >60%.

model adjustments were made with the interactive computer graphics program FRODO (Jones, 1978).

Because the resolution of the available diffraction data was insufficient to permit simultaneous refinement of both occupancy and thermal parameters for the atomic groups present in multiple discrete conformations, the weight assignments for these groups were made in relatively coarse steps based on the appearance of the difference density maps and the refined "omit" maps (Smith et al., 1988). The maps clearly indicated that the occupancies of certain multiple protein conformers systematically vary with pH, with one predominant position at low pH and an alternative position that becomes increasingly evident with increasing pH. These trends were reflected in the weight assignments to the partially occupied protein conformers.

The weight assignments for alternative protein conformations were not biased by assuming the same temperature factors for different conformers. Instead, we made the initial assumption that the correct B factors for a given conformer do not change with occupancy. After refinement, the B factors for the partially occupied "low-pH" and "high-pH" conformers at intermediate pH values remained similar to those obtained for the completely occupied conformations of these groups in the low- and high-pH structures.

For all atoms present in multiple conformations (with the single exception of the B chain COOH-terminal groups B29 Lys and B30 Ala) the individual atomic B factors did not significantly differ from the mean value of the protein. The errors in the weight assignments to the multiple protein conformers of cubic insulin are probably <30%.

The stereochemical parameters for the refined sodium-insulin models are given in Table 2. In addition to the detailed refinement of the models listed in Table 2, we also computed electron density maps from additional data (Table 1) for more qualitative comparisons.

RESULTS

We will divide the following section into two parts: first, a description of the observed structural changes in cubic insulin as a function of pH and ionic strength; and, second, correlations of these conformational changes with the titration of protein groups and on specific cation binding.

Structure of cubic insulin crystals as a function of pH and ionic strength

Electron density difference maps and comparisons of the refined atomic models at pH 7, 9, 10, and 11 show that the positions of most of the protein and well-ordered solvent atoms do not differ significantly among these structures. Local pH-dependent structural changes in cubic insulin (Fig. 1) are found in residues involved in two monovalent cation binding sites (Gursky et al., 1992), one interacting with the A5 Gln and the other involving B10 His; in the charged groups of the A chain NH_2 terminus and the B chain COOH-terminus; and in B25 Phe and the A chain COOH-terminal group A21 Asn.

Conformational changes in A5 Gln and cation binding between insulin dimers (region 1). In the insulin molecule, the A chain is C-shaped and consists of two helices, A1–A8 and A12–A21, connected by an extended chain. The cubic insulin crystal lattice is formed by rows of insulin dimers, with the antiparallel α-helical segments of the A chains from the neighboring dimers packed against each other and making end-to-end contacts between the dimers (Figs. 1 and 2, *b* and *c*) (Badger et al., 1991). A5 Gln and its symmetry mate across the crystallographic twofold axis are located near the interface between the insulin dimers.

At pH 7 in 0.1 M sodium, the major conformation of the A5 Gln side chain is oriented so that it may form hydrogen bonds with the OH group of A19 Tyr and either the A15 Gln side chain or the A1 Gly carbonyl oxy-

TABLE 2 **Summary of refinements of cubic bovine insulin structures under various solvent conditions**

pH	Na concentration	Resolution limit	R factor	rms deviations: From ideal covalent bond lengths	rms deviations: From distances determining angles	rms deviations: From planar peptide distances
	M	*Å*		*Å*	*Å*	*Å*
7	0.1	2.0	0.20	0.017	0.051	0.079
9	0.1	2.0	0.16	0.014	0.043	0.050
10	0.1	1.9	0.19	0.018	0.051	0.063
11	1.0	1.9	0.19	0.018	0.054	0.074

gen. When A5 Gln is in this position (designated "open"), the cleft created across the interface between the insulin dimers is filled by ordered water molecules forming a hydrogen-bonded network across the crystallographic dyad (Fig. 2, *a* and *b*).

At pH 9 in 0.1 M sodium, the predominant conformation of A5 Gln side chain is rotated by 180° about χ_1 so that it is oriented toward the dimer interface, replacing two water molecules and closing a cavity between the dimers ("closed" conformation [Fig. 2, *c* and *d*]). The remaining pair of the symmetry-related water molecules is replaced by a monovalent cation and an asymmetric pair of water molecules in the cavity, thus breaking the local crystal symmetry. The space vacated by the open A5 Gln conformer is filled by two ordered water molecules. At pH > 9 the closed conformation is the only position of A5 Gln that is seen in the map and the sodium occupancy is close to its maximal value of 0.5 (one cation per dyad). The conformational switching in A5 Gln is accompanied by 180° rotation of A9 Ser side chain around χ_1. Furthermore, the different conformations of the side chain of A5 Gln are associated with small shifts in the predominant positions of A15 Gln and A19 Tyr (which can only form hydrogen bonds to A5 side chain in the open conformation).

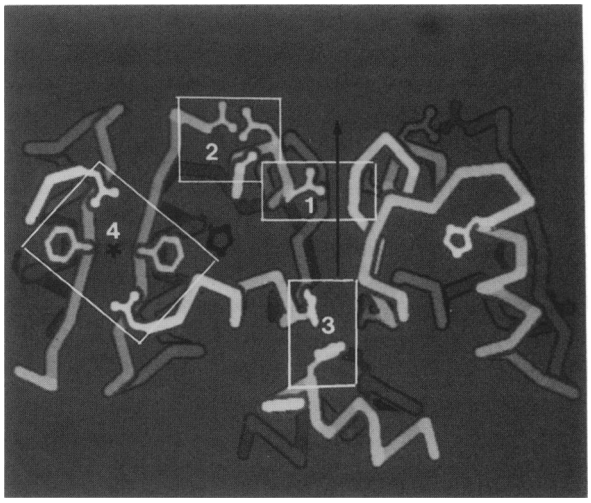

FIGURE 1 Crystal packing diagram of cubic insulin. The protein molecules are represented by a C_α atom chain trace with key side chains added. Regions of pH-dependent conformational changes are boxed: (*1*) cation binding site between the insulin dimers that involves A5 Gln; (*2*) interaction of A1 Gly with A4 Glu and B30 Ala; (*3*) cation binding site near B10 His, A14 Tyr; (*4*) switching of B25 Phe, A21 Asn, and their symmetry mates across the dimer twofold axis.

The structures of cubic bovine insulin in 0.1 M sodium at pH 7, 8, 9, and 10 indicate that the occupancies of the alternative A5 Gln conformers and the associated changes in the sodium occupancy at this site follow a normal titration curve with a midpoint at pH ~ 7.7. Increasing the sodium concentration from 0.1 to 1.0 M at pH 7 results in a change in the predominant position of the A5 Gln side chain from the open to the closed conformation and a comparable increase in the amount of bound sodium at this site. The structure near A5 Gln at pH 7 in 1 M sodium appears similar to the pH 8 structure in 0.1 M sodium. Thus, the midpoint of the pH-dependent conformational change in the position of A5 Gln is decreased by ~1 pH unit as a result of a 10-fold increase in sodium concentration.

Comparisons of the high-resolution sodium-insulin and potassium-insulin structures in 0.1 M cation concentration at pH 8, 9, and 10 showed that, under identical conditions of ionic strength and pH, the weights of the alternative A5 Gln conformers are similar. Consistent with the larger ionic radius of potassium compared with sodium ($r(K^+)$ = 1.33 Å, $r(Na^+)$ = 0.99 Å), the position of the bound potassium is slightly shifted from the sodium-binding site (Fig. 3). Absence of any significant features in the difference maps between the crystals grown with sodium or potassium and subsequently equilibrated against 0.1 M potassium salt solutions indicates complete occupancy by potassium at this site.

The cation binding site between the dimers is formed solely by protein carbonyl oxygens without close involvement of any charged or ionizable groups. The nearest ionizable amino acids A1 Gly α-amino group and B5 His are both ~7 Å away from the cation binding site.

Conformational changes in the charged groups A1 NH_2 terminus, A4 Glu, and B30 COOH terminus. At pH 7 in 0.1 M sodium or potassium, a terminal carboxyl oxygen from B30 COOH group and a side chain

carboxyl oxygen from A4 Glu are both involved in ionic interactions with the A1 Gly α-amino group from the same insulin molecule. At pH 8 in 0.1 M sodium or potassium, alternative conformers of A4 and B30 appear in the map, and at pH 9 in 0.1 M sodium or potassium these groups are clearly seen in two alternative positions (Fig. 4). At a higher pH, the separation between A4 COOH group and A1 α-amino group is increased from ~2.8 to ~4.5 Å. The two conformations of B30 COOH group are widely separated, but the atomic positions cannot be determined precisely since this group is very disordered in both conformations. At pH 10 in 0.1 M sodium, the high pH conformation of B30 COOH group becomes predominant, while the weights of the two A4 Glu conformers are approximately equal. Increase in sodium concentration from 0.1 to 1.0 M apparently stabilizes the low pH conformation of A4 carboxyl, which can be seen in the map even at pH 11. The position of A1 NH_2 terminus remains practically unaltered in the range of conditions studied.

B29 Lys is the most disordered residue in the structure and occupies more than one conformation at any pH. One of the lysine conformers is folded toward B21 Glu from the other insulin molecule within the molecular dimer, and this glutamic acid is also disordered at any pH. The shifts in the predominant positions of B29 Lys and B21 Glu are apparently coupled to the pH-dependent shift in the main chain atoms of B30 Ala.

Conformational changes in the cation binding site involving B10 His and A14 Tyr (region 3). At pH 7 in 0.1–1.0 M Na or K the major conformation of B10 His side chain is nearly parallel to the side chain of A14 Tyr from a neighboring insulin molecule (Fig. 5 *b*). In the alternate position, the histidine side chain is rotated away from the protein by about 120° in χ_1, vacating the site for monovalent cation binding (Gursky et al., 1992). Both histidine positions are occupied with approximately equal weights between pH 8 and pH 9 in 0.1–1.0 M sodium or potassium (Fig. 5 *a*), but at pH $\geq$ 10 in 0.1–1 M sodium the conformation that vacates the cation binding site becomes predominant (Fig. 5 *c*). Associated with this conformational switch are small pH-dependent shifts in the position of the side chain of A14 Tyr. Additional well-ordered water molecules are seen in the maps near the OH group of A14 Tyr at pH $\geq$ 10.

Conformational switching of B25 Phe and A21 Asn at pH 11 (region 4). At pH 11 in 1 M sodium, the A chain COOH-terminal residue A21 Asn is disordered into two closely spaced conformations, and an additional conformation of the side chain of B25 Phe flipped across the molecular dimer interface is observed (Fig. 6). The two conformations of B25 Phe and A21 Asn have equal weights at pH 11. The conformational switching in B25 Phe breaks the local symmetry of the crystallographic insulin dimer and is apparently coupled to the shifts in the position of A21 Asn since the B25 Phe position across the dimer twofold axis is incompatible with the single A21 Asn conformation observed at pH < 11 (Fig. 6, *b* and *c*). The two alternative positions of B25 Phe and A21 Asn observed at pH 11 resemble the structures of the two independent molecules in the 2Zn insulin crystal dimer at pH 6.3.

The B25 Phe conformation folded across the dimer symmetry axis is not seen at pH 7–10 in any salt concentration. Thus, the conformational change in B25 Phe in cubic insulin crystals is apparently driven by the increase in pH rather than the ionic strength. Additional well-ordered water molecules observed in the map in the region of B25 Phe and A19 Tyr probably indicate ionization of A19 Tyr at pH $\geq$ 10.

Other amino acids. Several single amino acid residues, including A18 Asn, B3 Asn, and B22 Arg, exhibit pH-dependent discrete disorder, while several other protein groups, including B4 Gln, B21 Glu, and B29 Lys, are present in more than one conformation at any pH. In total, 16 of the 51 insulin residues were modeled in multiple conformations, with the weights of most of them varying over the pH range 7–11. These residues are A4 Glu, A5 Gln, A9 Ser, A14 Tyr, A15 Gln, A18 Asn, A19 Tyr, A21 Asn (A chain COOH-terminal), B3 Asn, B4 Gln, B10 His, B21 Glu, B22 Arg, B25 Phe, B29 Lys, and B30 Ala (B chain COOH-terminal). In at least one of their conformations these groups are accessible to solvent and, with the single exception of B25 Phe, are charged or polar. Analysis of the 2.5 Å x-ray data collected from a crystal at pH 6.5 in 0.1 M sodium salt suggests conformational changes in B1-B3 segment.

In cubic insulin crystals the three copies of the B chain α-amino groups related by the threefold symmetry axis are separated from each other by 6.7 Å. In contrast to the conformational changes observed between pH 8 and 10 near the α-amino group from A1 Gly, the protein and well-ordered solvent structure near the three copies of the B1 Phe α-amino groups are conserved over the pH range 7–11 (Fig. 7). B1 Phe, B17 Leu, B18 Val, and their symmetry mates across the crystal threefold axis form a hydrophobic crevice containing three large symmetry-related solvent density peaks near the center of the trigonal crevice. The centers of these density peaks are within hydrogen-bonding distances from each other but make no close contacts to any protein atoms.

In cubic insulin crystals, B5 His is located at the protein surface and is not involved in direct interactions with any ionizable protein groups or cations. In contrast to the conformational switching observed in B10 His between pH 7 and 10, the protein and well-ordered solvent structure in the vicinity of B5 His appears invariant over the pH range 7–11.

Specific binding of dichloroethane to insulin dimer. All crystals in the pH range 7–11 treated with Formvar solution in dichloroethane contained a dichloroethane molecule bound in a hydrophobic cavity formed by B12

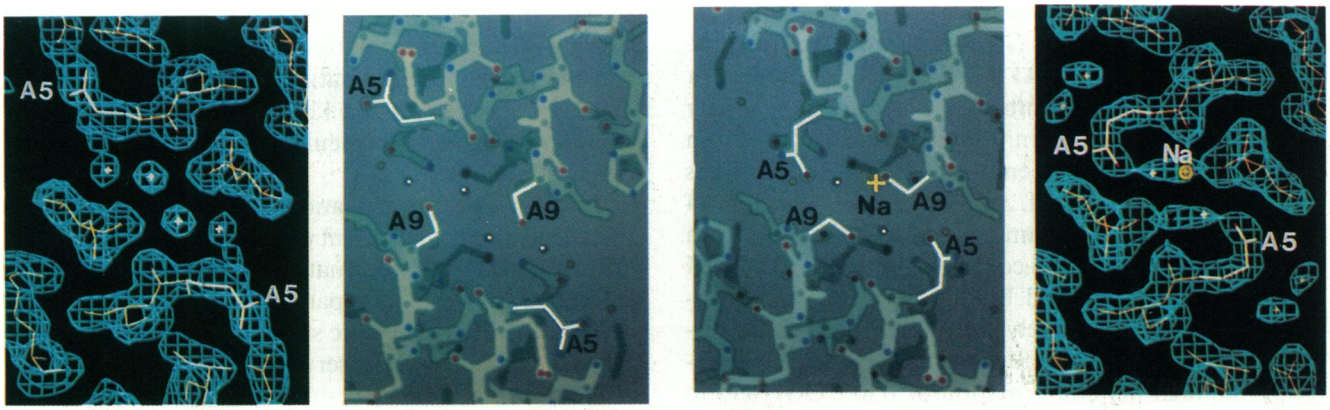

FIGURE 2, *a, b, c,* and *d*

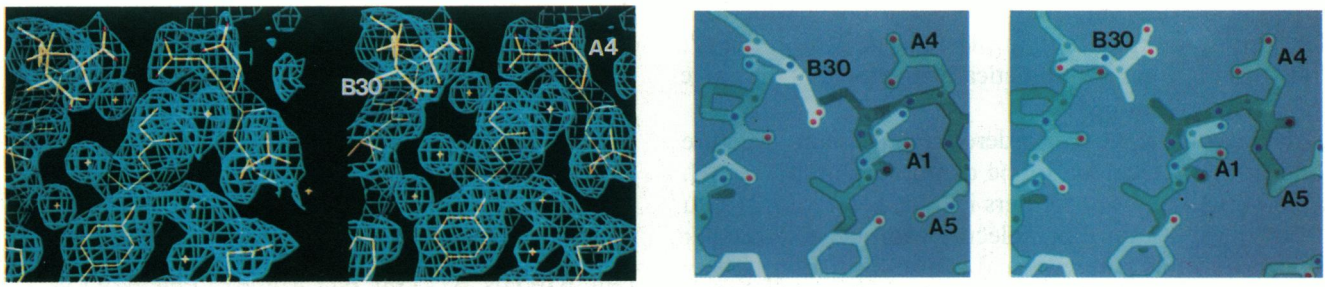

FIGURE 3, *a, b,* and *c*

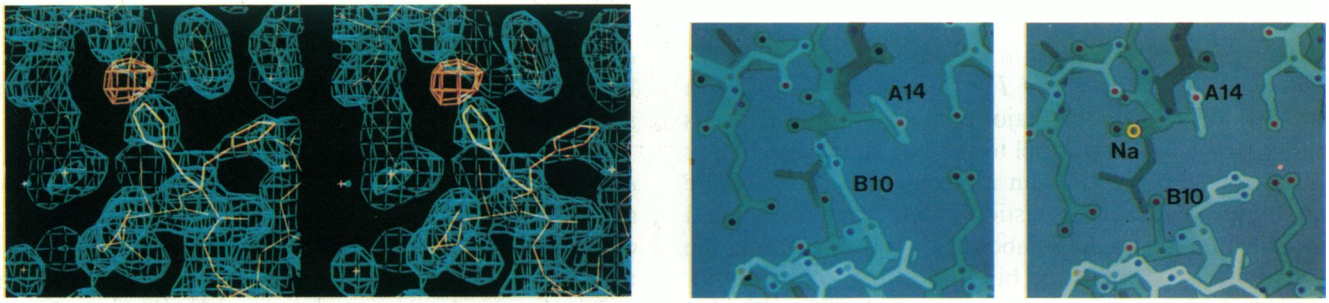

FIGURE 4, *a, b,* and *c*

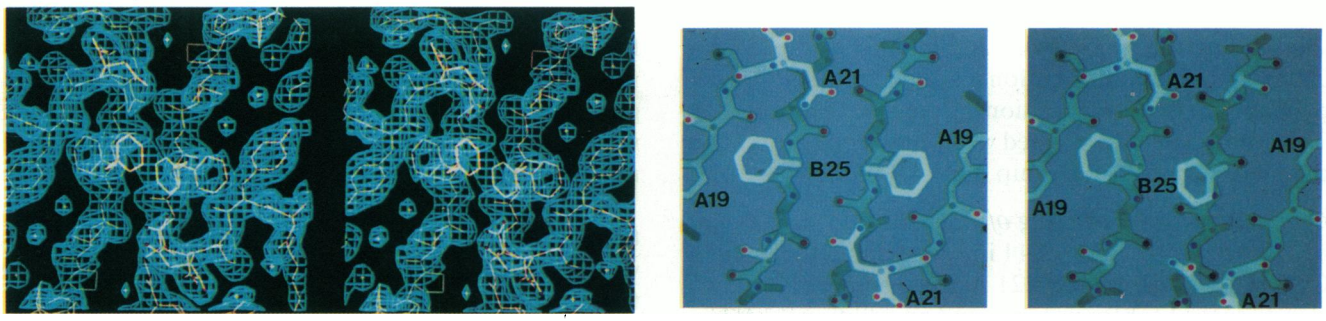

FIGURE 5, *a, b,* and *c*

FIGURE 2 A conformational change in A5 Gln gates cation binding between the insulin dimers. (*a*) Electron density map at pH 7 in 0.1 M sodium shows A5 Gln in the open conformation (viewed approximately along the crystal twofold axis). Four spherical density peaks in the cleft between the insulin dimers represent well-ordered water molecules hydrogen-bonded to each other and to the protein carbonyl oxygens. The map was computed using coefficients $2F_{obs} - F_{ref}$, where F_{obs}'s were measured at pH 7 in 0.1 M sodium, F_{ref}'s were obtained from the refined model at pH 7 in 0.1 M sodium, and phases were computed from the same model. (*b*) Model representation of the open cleft between the insulin dimers (viewed approxi-

Val, B16 Tyr, and their symmetry mates across the dimer twofold axis. The dichloroethane molecule is bound in a symmetric position in a staggered conformation, with its dipole moment parallel to the electric field created along the dimer twofold axis by the two copies of B13 Glu. The dichloroethane occupancy in all crystals is close to its maximal possible value of 0.5 (i.e., one dichloroethane molecule per insulin dimer). Bound dichloroethane has only a minor effect on the protein and solvent structure in the cavity, and the structure remains essentially conserved in the pH range 8–11. Other halogenated methane, ethane, and ethylene compounds can also bind at this site with high specificity (work in progress).

Correlation of conformational changes with specific cation binding and titration of protein groups

Variations in pH from 7 to 11 result in titration of certain insulin groups and induce local structural changes in the protein and solvent. The variable parts of the structure are seen in multiple discrete positions, with the relative weights of alternative conformers systematically varying with pH. Some of these changes, like the rotation of B10 His or shifts in the relative positions of the B chain COOH-terminal and the A chain NH_2-terminal groups, may be accounted for by titration of residues that interact directly with the variable conformers. These conformational changes can, therefore, be used for estimates of the pK values of these residues in cubic insulin crystal. Other substantial pH-dependent changes, such as the movements of A5 Gln or B25 Phe, are not directly linked to titrating protein groups in any obvious way.

Conformational switching of A5 Gln gates monovalent cation binding. Conformational switching of A5 Gln and A9 Ser is coupled to monovalent cation binding between the dimers. The closed glutamine and serine conformation form a cavity on the crystal dyad, which is not directly accessible to solvent. The cavity contains a bound sodium ion and associated water molecules in one of two symmetry-related sets of positions, so the observed average crystal structure possesses twofold symmetry. When the A5 Gln side chain is rotated in the open position, it displaces well ordered water and makes hydrogen bonds to A19 Tyr phenolic oxygen, A15 Gln side chain oxygen, or A1 Gly carbonyl oxygen, while the space vacated by the closed glutamine conformation is filled by two ordered waters. Thus, the cavity between the insulin dimers becomes solvent accessible and the cation is displaced by water. The cleft between insulin dimers is filled by a continuous hydrogen-bonded network of ordered water molecules.

At high pH, more positive counterions are required to neutralize the increased net negative charge on the protein. Therefore, an increase in pH and/or in the solvent cation concentration would be expected to induce conformational changes in the protein that would facilitate increased cation binding. This proved to be the case for the cation binding site between the insulin dimers. The equilibrium between the open and closed conformations

mately along the crystal twofold axis). Six hydrogen-bonded water molecules and their symmetry mates are shown in the cleft (*yellow circles*). The open A5 Gln conformation is predominant at pH 7 in 0.1 M sodium salt. (*c*) Model representation of the cavity between the insulin dimers formed by the closed conformation of A5 Gln. The cavity contains a bound sodium ion and two water molecules. The closed A5 Gln conformation becomes predominant as pH is raised from pH 7 to pH 9 and/or as salt concentration is increased from 0.1 to 1 M. (*d*) Electron density map of sodium insulin (0.1 M sodium, pH 9) shows A5 Gln in the closed conformation. Symmetry-related density peaks in the cavity represent the symmetry-averaged structure of bound sodium and water. The map $2F_{obs} - F_{ref}$ was computed with amplitudes F_{obs} measured from the crystal at pH 9 in 0.1 M sodium, and F_{ref} and phases obtained from the refined model at pH 9 in 0.1 M sodium.

FIGURE 3 Conformational changes in A4 Glu and B30 COOH group interacting with A1 α NH_2 group. (*a*) Stereopair electron density map of the pH 9 structure in 0.1 M sodium shows two sets of alternative conformations of A4 Glu and B30 Ala and a single conformation of A1 Gly. B29 Lys and B30 Ala are the most disordered residues in cubic insulin. Their B factors at any pH are about three times larger than the mean value. Therefore, the density for the partially occupied conformers of B30 Ala at pH 9 in 0.1 M sodium is relatively weak. At pH 7 and pH 10 in 0.1 M sodium, when only one of the two alternative alanine positions is seen in the map, the density appears somewhat stronger. (*b*) Model structure at pH 7 in 0.1 M sodium shows A4 Glu and B30 Ala carboxyls interacting with the A1 Gly α-amino group. (*c*) Model representing the alternative positions of A4 Glu and B30 Ala observed at pH > 8 in 0.1 M sodium. At a higher pH, A4 Glu COOH group is shifted away from A1 α NH_2 group.

FIGURE 4 B10 His competes with a cation for a binding site. (*a*) Stereopair electron density map at pH 9 in 0.1 M sodium showing two alternative positions of B10 His. Both positions have almost equal occupancy in the pH range from 8 to 9. The superimposed difference density peak (*orange*) between Tl-insulin and sodium-insulin crystals (0.1 M salt, pH 9) indicates that a Tl binding site overlaps with one of the B10 His conformations (Gursky et al., 1992). (*b*) Model representation of the pH 7 structure (0.1 M sodium) showing B10 His nearly parallel to A14 Tyr. This histidine conformation occludes the cation binding site. (*c*) Model representation of the pH 10 structure in 0.1 M sodium. B10 His side chain is rotated $\sim 120°$ in χ_1 in the alternative conformation. The space vacated by the histidine ring can be occupied by a monovalent cation.

FIGURE 5 Conformational changes in B25 Phe and A21 Asn observed at pH 11 in 1 M sodium. (*a*) Stereopair electron density difference map $2F_{obs} - F_{ref}$ at pH 11 in 1 M sodium showing alternative conformations of B25 Phe and A21 Asn viewed along the dimer twofold axis. (*b*) Model representation of B25 Phe and A21 Asn conformations at pH < 11. In the cubic crystal, the two molecules within an insulin dimer are related by a crystallographic twofold symmetry axis. At pH 7–10, B25 Phe side chains are oriented away from the dimer twofold axis, resembling the structure of molecule 1 from the 2Zn insulin dimer. (*c*) Model representation of pH 11 structure in 1 M sodium. Two alternative sets of conformations are observed in B25 Phe and A21 Asn (A chain COOH-terminal). The new conformations of these groups break the local crystal symmetry and are similar to those found in molecule 2 in the 2Zn insulin crystal.

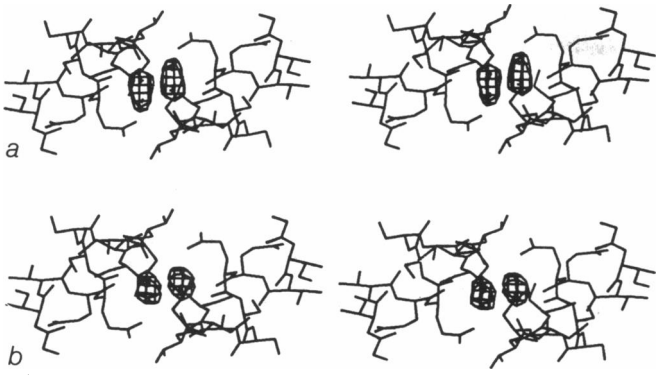

FIGURE 6 Difference maps for sodium (*top*) and potassium (*bottom*) bound in the cavity between insulin molecules. (*a*) Difference density map $F_{Na} - F_{omit}$ between the data collected from sodium-insulin crystal (0.1 M Na, pH 9) and the model from which the contents of the cavity between the insulin dimers were omitted. This map, computed using the phases from this "omit" model, shows the symmetry-averaged density distribution of the sodium and water bound in the cavity formed by the closed A5 Gln conformation. Initially, this density was interpreted as a sodium + water pair (Gursky et al., 1992). The density peaks appear elongated since Na^+ (r = 0.99 Å) can approach carbonyl oxygens from A5 Gln and A10 Ile closer than the water (r = 1.4 Å) from the symmetry-related site. Computer simulations of Na^+ binding in this cavity (Badger, J., unpublished results) and individual B factor and occupancy refinement of Na and water now indicate that sodium is coordinated by two water molecules and two carbonyl oxygens. This model accounts for the unequal distribution of density in each lobe of the elongated peak, corresponding to the average about the twofold axis of one sodium atom on one side and two water molecules on the other. (*b*) A similar difference density map with coefficients $F_K - F_{omit}$ for crystals equilibrated with 0.1 M potassium shows a K^+ ion and a water molecule bound between the dimers. The density peaks appear nearly spherical since, due to similarity in the radii of potassium ($r(K^+)$ = 1.33) and water, the distances of their approach to protein oxygens are similar. Thus, their positions are overlapped. Because the potassium ion is larger than sodium, there is space for only a single coordinating water molecule in the cavity.

of A5 Gln depends on pH and monovalent cation concentration, with the weight of the closed conformation increasing with an increase in pH and cation concentration. In 0.1 M sodium the conformational switching of A5 Gln and A9 Ser follows a normal titration curve with a midpoint around pH 7.7, while in 1 M sodium the midpoint for switching, if the crystals were stable in acidic solution, would be below pH 7.

Interactions of Na^+ and hydronium ions with proteins have not been directly documented by crystallographic methods because of similarity in the scattering factors of Na^+ (10 electrons), hydronium ion (10 electrons), and water (10 electrons). In cubic insulin, however, several observations unambiguously indicate sodium binding at the site between the dimers. In our previous work, the presence of small monovalent ions proved to be essential for crystal stability. Isomorphous replacement of sodium by the heavy cations rubidium and thallium was used to identify sodium positions in cubic insulin, and potassium and lithium were also found to bind at the same sites (Gursky et al., 1992). The pH-dependent changes in thallium occupancy at the site between the dimers correlate with the results presented here on pH-dependent switching of A5 Gln in sodium-insulin crystals. Furthermore, after refinement without restraining contact distances, the sodium ion was located 2.3 Å away from the carbonyl oxygens of A5 Gln and A10 Ile, which is a normal contact distance for sodium-oxygen, but is ~0.5 Å less than the water oxygen or hydronium-oxygen distances. Finally, the fact that at pH 7 an increase in sodium concentration from 0.1 to 1 M (without changing the hydronium ion concentration or the water activity) shifts the equilibrium in A5 Gln and A9 Ser from the predominantly open to the closed position provides additional evidence of sodium binding at this site.

Comparison of the weights of alternative A5 Gln and A9 Ser conformers at different pH and sodium salt concentrations provides an estimate of the binding constant for sodium ion as a function of pH. The weight of the closed glutamine conformation is apparently ~0.3 at pH 7 in 0.1 M sodium, and is >0.7 at pH 7 in 1 M sodium (Table 3). At a sodium concentration between 0.3 and 0.6 M the weights of the open and closed conformations are equal and the site is half occupied; thus, the binding constant for sodium at pH 7 is K (pH 7) ~ 2–3 (M^{-1}). At pH 8 in 0.1 M sodium, the site occupancy is ~0.7 and the estimated binding constant at this pH is K (pH 8) ~ 20–30 (M^{-1}). An approximately 10-fold increase in the binding constant for sodium with a 10-fold decrease in the free proton concentration indicates that sodium binding at this site is correlated with proton dissociation somewhere else on the protein and follows the mass action law. Comparison of high-resolution structures of sodium-insulin and potassium-insulin showed

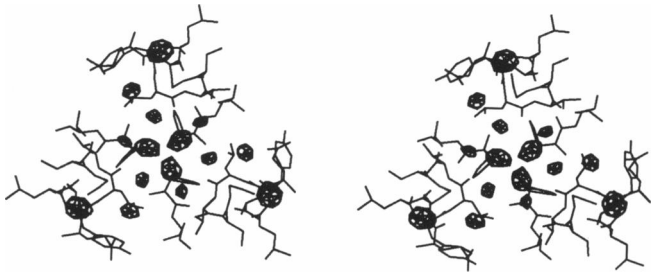

FIGURE 7 Stereopair of the electron density difference map showing protein and well-ordered solvent structure near the three copies of the B chain NH_2 termini B1 Phe. The map with coefficients $F_{obs} - F_{omit}$ was computed between the data at pH 9 in 0.1 M sodium and the relevant refined model from which five water molecules located near the threefold axis were omitted. The phases were obtained from the same model. Three large oblate symmetry-related density peaks are located at the bottom of a hydrophobic crevice ~ 3 Å from each other but make no close contacts to any protein atoms. They probably represent water positions in which any two water molecules may be hydrogen-bonded to each other. Smaller density peaks correspond to less well-ordered waters, making hydrogen bonds to each other and/or to the protein atoms. The protein and solvent structure in this region is conserved in the pH range 7–11 in 0.1–1 M salt.

TABLE 3 **Relative weights of multiple protein conformers at different pH and solvent cation concentrations for protein groups from four regions: (1) A5 Gln and A9 Ser that gates cation binding in the cavity between the insulin dimers; (2) A4 Glu and B30 Ala carboxyls interacting with A1 Gly α-amino group; (3) B10 His that can compete for a binding site with a cation; (4) B25 Phe and A21 Asn paired across the dimer dyad**

Cation concentration	pH	Regions with variable weights of alternate protein conformers							
		A5 Gln, A9 Ser-cavity		B30, A4 Glu, A1 α-amino		B10 His-Na^+ site		B25 Phe, A21 Asn
M								
0.1 Na or K	7	Open Closed	0.7 0.3	Low pH	1.0	Occluded	>0.7	Symmetric
	8	Open Closed	0.3 0.7	Low pH High pH	0.7 0.3	Occluded Vacated	0.6 0.4	Symmetric
	9	Closed	>0.7	Low pH High pH	0.6 0.4	Occluded Vacated	0.5 0.5	Symmetric
	10	Closed	1.0	High pH	1.0	Vacated	>0.7	Symmetric
1.0 Na	7	Closed	>0.7	Low pH	1.0	Occluded	>0.7	Symmetric
	9	Closed	1.0	Low pH	>0.7	Occluded Vacated	0.5 0.5	Symmetric
	11	Closed	1.0	High pH	0.7	Vacated	1.0	Asymmetric

that, under identical conditions of pH and salt concentration, the weights of the alternative A5 Gln and A9 Ser conformers are similar, indicating similar (but not necessarily identical) binding constants for Na^+ and K^+.

Conformational changes in A4 Glu and B30 COOH terminus are linked to titration of the A1 Gly α-amino group. At pH 7, the α-amino group from A1 Gly is involved in ionic interactions with two carboxyl groups from A4 Glu and B30 Ala (the B chain COOH terminus). Increased separation between A4 carboxyl and A1 NH_2 group observed at pH ≥ 9 is apparently due to the deprotonation of the A1 α-amino group. Judging from the relative weights of the alternative conformers of B30 Ala and A4 Glu between pH 7 and 10, the pK of this α-amino group is close to 9 in 0.1 M sodium salt solution. The somewhat elevated pK of this amino group compared with its normal value in the pH range 7.9–8.6 is probably due to the electrostatic interactions with the negatively charged carboxyls from A4 Glu and B30 COOH group.

Increased salt concentration enhances shielding of the negative charges from B30 COOH group and A4 Glu. As a result, the low-pH configuration of these groups is stabilized by increasing the sodium salt concentration from 0.1 to 1 M (Table 3).

B10 His competes with monovalent cations for a binding site. The monovalent cation binding site associated with B10 His provides another example of the pH-dependent conformational changes that facilitate increased cation binding at higher pH. Shift in the B10 His side chain from the predominantly occluding position to the conformation that vacates the site for a cation binding occurs as the pH is raised from 7 to 10, with the weights of the two histidine conformers being nearly equal in the pH range from pH 8 to pH 9. A plausible interpretation of this behavior is that B10 His titrates with an anomalously high pK of 7.5 compared with the normal pK ~ 6. The elevated pK of this histidine results from the electronegative potential at the cation binding site which is created by combined action of the peptide unit dipoles and by the neighboring A17 Glu. At pH 7, B10 His is probably largely protonated and is found almost entirely in the position that occludes the cation binding site. In the pH range 8–9, B10 His is probably largely neutralized and occupies two alternative positions with nearly equal probability. A further increase to pH 10 leads to deprotonation of A14 Tyr, which increases the site affinity for a positive charge. As a result, at pH ≥ 10 the neutral histidine is largely displaced by a cation from the binding site and is seen predominantly in the nonoccluding conformation. The substantial increase in the cation occupancy measured with Tl^+ between pH 9 and 10.5 (Gursky et al., 1992) can be accounted for by the deprotonation of A14 Tyr in this pH range.

Alternative conformations of B25 Phe and A21 Asn in cubic insulin at pH 11 resemble conformations of these groups in 2Zn insulin crystals at pH 6.3. B25 Phe and A21 Asn (A chain COOH-terminal) are among the residues involved in the formation of the insulin dimer and in insulin receptor binding (Baker et al., 1988). These groups are present in differing conformations in the two independent molecules of the 2Zn insulin dimer at pH 6.3, with the B25 Phe side chain folded back across the protein in molecule 1 and folded over the quasi-twofold dimer axis in molecule 2. The conformation of B25 Phe

TABLE 4 **Estimated pK values of the ionizable groups with pK > 6 in cubic insulin crystals in 0.1 M sodium salt**

Sequence number	Ionizable group	pK	Rationale
B5	His	~6	Assumed to be normal
B10	His	7.5	Inferred from the occupancies of the alternative histidine conformations at different pH
A1	α-NH_3	~9	Inferred from the occupancies of the alternative conformers of A4 Glu and B30 Ala at different pH
B1	α-NH_3	6–10	Close apposition of 3 α-amino groups would lower the first pK and raise the third pK
A14	Tyr	~10	From changes in cation occupancy at the site alternatively occupied by B10 His
A19 B16 B26	Tyr	10.5	Assumed to be same as in solution as measured by spectrophotometric titration
B29	Lys	10.5	Assumed to be normal
B22	Arg	12.5	Assumed to be normal

seen in molecule 2 is predominant in the insulin monomer in solution and probably depicts the position of this group in the course of the insulin receptor binding (Shoelson et al., 1992). In the exact crystallographic dimer of cubic insulin at pH < 11, conformations of B25 Phe and A21 Asn are similar to those of molecule 1. At pH 11, these groups are present in two equally occupied conformations similar to the positions of molecule 1 and molecule 2 in 2Zn insulin crystals. The conformational switch involving B25 Phe and A21 Asn in cubic insulin is not obviously linked to titration of particular protein groups. It is possible that the folded-over B25 Phe side chain conformation observed at pH 11 is correlated with ionization of the neighboring A19 Tyr.

Other protein groups. Titration of protein groups is not invariably accompanied by observable structural changes in their vicinity (Dixon et al., 1991). Therefore, an absence of pH-dependent structural changes in the protein and solvent near the three copies of B1 Phe amino groups, near B5 His, and near B16 and B26 tyrosines does not necessarily imply that charges on these groups remain unaltered over the pH range 7–11.

Charge on the insulin molecule as a function of pH. The charge on the insulin molecule as a function of pH can be estimated using the approximate pK values estimated for the ionizable groups in cubic insulin (Table 4). At pH 7, the A and B chain COOH-termini and the side chain COOH of A4, A17, B13, and B21 Glu should be negatively charged, B5 His is probably partially or largely deprotonated, B10 His largely protonated, A1 positively charged, B1 probably partially deprotonated, A14, A19, B16, and B26 Tyr neutral, and B29 Lys and B22 Arg positively charged. Thus, at pH 7 the negative net charge on the insulin monomer in the cubic crystal form is between −1 and −2. At pH 10, B5 and B10 histidines and both NH_2 termini should be neutral, the four tyrosines partially deprotonated, B29 Lys partially or largely protonated, and B22 Arg positively charged. Thus, the negative net charge on the insulin molecule at pH 10 is probably between −5 and −6.

DISCUSSION

Protein plasticity

The A chain NH_2-terminal segment plays an important role in the insulin receptor interaction. Shifts in the relative positions of the A chain NH_2-terminal and the B chain COOH-terminal groups observed in cubic insulin at alkaline pH may be indicative of the separate positions of these groups required for the insulin receptor binding (Derewenda et al., 1991; Hua et al., 1991).

Probable participation of glutamine side chains in ion channel gating has been suggested for the ion channel peptides alamecitin (Fox and Richards, 1982) and [Leu^1]-zervamicin (Karle et al., 1991), based on positions and/or increased mobilities of certain glutamine groups in the crystals of these antibiotics. Karle et al. (1991) suggested that probably "one of the distinctive functions of the glutamine residue is in regulation of ion-transport peptides." Glutamine-gated ion binding in cubic insulin provides an experimental example of how a glutamine side chain may be involved in the regulation of monovalent cation binding.

Linkage between conformational changes

Comparison of cubic insulin structures at different solvent conditions indicates that pH-dependent conformational changes are linked within the regions of directly interacting protein groups and solvent atoms. These regions include (*1*) A5 Gln, A9 Ser, A15 Gln, A19 Tyr, A1 Gly, cation, ordered water; (*2*) A1 Gly, A4 Glu, B30 Ala, B29 Lys, B21 Glu; (*3*) B10 His, A14 Tyr, cation, ordered water; and (*4*) B25 Phe, A21 Asn.

In region 1, for example, switching of the A5 and A9 side chains from the open to the closed conformation is coupled to cation binding between the dimers and can be induced by an increase in pH from 7 to 9 in 0.1 M salt, as well as by an increase in the salt concentration from 0.1 to 1 M at pH 7. The change in the position of A5 Gln is also coupled to small conformational shifts in A15 Gln and A19 Tyr side chains, which can make hydrogen bonds to the open conformer of A5 Gln. However, the position of A1 Gly is unaffected by possible hydrogen bonds between the carbonyl oxygen to the open A5 Gln conformer.

In region 2, ionic interactions connecting the α-amino group from A1 Gly to the carboxyls from A4 Glu and

B30 COOH terminus weaken as this amino group is being titrated in low ionic strength solution, which results in shifts in the positions of A4 Glu and B30 Ala. Increasing the salt concentration from 0.1 to 1 M in sodium enhances shielding of the negatively charged carboxyls and stabilizes the ionic interactions connecting them to the A1 Gly α-amino group.

In contrast to correlated shifts in the positions of the directly interacting residues, conformational changes in relatively remote groups are not strongly correlated (Table 3). For example, in 0.1 M sodium the midpoint of transition between the alternative A5 Gln conformations in region 1 is pH $\sim$ 7.7, whereas the A1 Gly α-amino group, which is $\sim$7 Å distant from A5, has a pK $\sim$ 9 as inferred from the pH-dependent change in carboxyl group positions in region 2. Furthermore, increasing the salt concentration from 0.1 to 1 M reduces the midpoint for the A5 Gln structural transition to below pH 7, but apparently increases the midpoint of the conformational shifts in A4 and B30 carboxyls to a pH of $\sim$10. Thus, there is no evident linkage between A5 Gln conformational switching and A1 Gly titration or titration of any other single insulin group. It appears that the cation binding near A5 Gln is loosely coupled to changes in the protonation of more than one protein group.

Comparison of structural changes in other regions under a variety of solvent conditions (Table 3) indicates that these changes are not triggered by a single conformational switch or titration of a particular protein group. Thus, conformational pH-dependent changes in different regions of the cubic insulin structure appear to be only loosely coupled. From the crystal structures of insulin hexamers, Chothia et al. (1983) speculated that asymmetry in the orientations of the two copies of B25 Phe of the dimer interface was the result of conformational changes propagating $\sim$20 Å from the A chain N-terminal helix. In cubic insulin crystals at pH 11, the asymmetry we observe in B25 Phe is only coupled to conformational changes in the neighboring residue A21 Asn, which suggests that the reorientation of B25 Phe is the result of local forces. Consistent with this interpretation, a variety of experimental results (Caspar and Badger, 1991) now indicate that most of the intrinsic flexibility in hydrated proteins at room temperature is due to independent movements of small groups of atoms rather than rigid-body movements or long-range elastic coupling.

Conformational heterogeneity and protein dynamics

Conformational heterogeneity involving 6–13% of the amino acid groups was reported for several highly refined protein structures (Smith et al., 1986; Swensson et al., 1987); and in the erabutoxin structure refined to 1.4 Å resolution (Smith et al., 1988), 22% of the protein groups were modeled in multiple alternative positions. The question was raised whether multiple conformations exist dynamically in these crystals or are due to static lattice disorder. Our analyses of cubic insulin at room temperature show that, in response to variations in the pH and solvent ion concentration, the crystal structure travels between stable substates by changing the weights of the alternative atomic positions. Thus, the equilibrium between these substates at room temperature is apparently dynamic. The conformational variations that we have mapped in $\sim$30% of the insulin amino acid residues in the pH range 7–11 are probably facilitated by the low ionic strength conditions and may also reflect the fact that the relatively large proportion of residues in the small insulin molecule is accessible to the solvent in the cubic crystal form.

Zinc-containing insulin crystals, which are composed of insulin hexamers rather than dimers, provide another interesting system for experimental studies of electrostatic interactions, but are likely to be only stable over a narrower range of pH around neutrality.

We focused on the effect of electrostatic interactions, particularly pH and salt concentration, on cubic insulin conformations. Among other factors that may affect conformational equilibria in protein crystals are packing constraints for particular crystal forms (Badger, 1992), solvent composition, temperature, pressure, and ligand binding. Variations in different factors (such as pH and packing constraints) can stabilize similar protein conformations: for example, two alternative positions of B25 Phe and A21 Asn found in cubic insulin at pH 11 are similar to the conformations of these groups in the two independent molecules of the 2Zn insulin dimer at pH 6.3. A similar conformational response to various external factors suggests that the number of stable protein conformations is limited and that conformational substates of insulin in solution would include those found in crystalline forms under a variety of solvent conditions (Hua et al., 1991).

The plasticity of insulin structures, which is evident from crystallographic analyses of cubic insulin crystals in different solvent conditions, illustrates the intrinsic adaptability of protein structures (Caspar and Badger, 1991). For example, the pH-dependent cation binding in the cavity of the insulin dimer resembles the behavior of the postulated voltage-gated ion channels (Eisenman and Dani, 1987). The conformational switching in insulin crystals has no evident physiological significance, but displays the potential of protein structures to adapt to changes in physiological environment.

The refined coordinates of the cubic bovine sodium-insulin structures at pH 7, 9, and 10 in 0.1 M sodium, and at pH 11 in 1 M sodium have been deposited with the Protein Data Bank.

Kinemages

The kinemage program, developed by D. C. and J. S. Richardson (1992), presents a unique means in commu-

nicating the three-dimensional structure of cubic insulin to the reader. The current version of MAGE allows the user to read in coordinates with standard Brookhaven format and display numerous aspects of the structure through use of color, rotation, and a simple animation. The kinemages produced by Eric Fontano for this article are found with the MAGE program on the Macintosh disk accompanying the journal. Through these graphic images, one can directly observe the conformational changes of the four specified regions in the cubic insulin crystal.

We are very grateful to E. Fontano for his help with the preparation of the kinemage, and to R. Diaz-Avalos for growing potassium-insulin crystals.

This work was supported by National Institutes of Health grant CA-47439, awarded to D. L. D. Caspar by the National Cancer Institute. Grant BBS-8713278, awarded to K. Kalata by the National Science Foundation, supported the development of the Brandeis area detector.

Received for publication 27 April 1992 and in final form 4 June 1992.

REFERENCES

Agarwal, R. C. 1978. A new least-squares refinement technique based on the fast Fourier transform algorithm. *Acta Crystallogr.* A34:791–809.

Badger, J. 1992. Flexibility in crystalline insulins. *Biophys. J.* 61:816–819.

Badger, J., and D. L. D. Caspar. 1991. Water structure in cubic insulin crystals. *Proc. Natl. Acad. Sci. USA.* 88:622–626.

Badger, J., M. R. Harris, C. D. Reynolds, A. C. Evans, E. J. Dodson, G. G. Dodson, and A. C. T. North. 1991. Structure of the pig insulin dimer in the cubic crystal. *Acta Crystallogr.* B47:127–136.

Baker, E. N., T. L. Blundell, J. F. Cutfield, S. M. Cutfield, E. J. Dodson, G. G. Dodson, D. C. Hodgkin, R. E. Hubbard, N. W. Isaacs, C. D. Reynolds, K. Sakabe, and N. Vijayan. 1988. The structure of 2Zn pig insulin crystals at 1.5 Å resolution. *Philos. Trans. R. Soc. Lond. B. Biol. Sci.* B319:369–457.

Caspar, D. L. D., and J. Badger. 1991. Plasticity of crystalline proteins. *Curr. Opin. Struct. Biol.* 1:877–882.

Chothia, C., A. M. Lesk, G. G. Dodson, and D. C. Hodgkin. 1983. Transmission of a conformational change in insulin. *Nature (Lond.).* 302:500–505.

Derewenda, U., Z. Derewenda, E. J. Dodson, G. G. Dodson, X. Bing, and J. Marcussen. 1991. X-ray analysis of the single chain B29-A1 peptide-linked insulin molecule. *J. Mol. Biol.* 220:425–433.

Dixon, M. M., R. G. Brennan, and B. W. Matthews. 1991. Structure of γ-chymotrypsin in the range pH 2.0 to pH 10.5 suggests that γ-chymotrypsin is a covalent acyl-enzyme adduct at low pH. *Int. J. Biol. Macromol.* 13:89–96.

Dodson, E. J., G. G. Dodson, A. Lewitova, and M. Sabesan. 1978. Zinc-free cubic pig insulin: crystallization and structure determination. *J. Mol. Biol.* 125:387–396.

Eisenman, G., and J. A. Dani. 1987. An introduction to molecular architecture and permeability of ion channels. *Annu. Rev. Biophys. Biophys. Chem.* 16:205–226.

Fox, R. O., and F. M. Richards. 1982. A voltage-gated ion-channel model inferred from the crystal structure of alamethicin at 1.5-Å resolution. *Nature (Lond.).* 300:325–330.

Gursky, O., Y. Li, J. Badger, and D. L. D. Caspar. 1992. Monovalent cation binding to cubic insulin crystals. *Biophys. J.* 61:604–612.

Guss, J. M., P. R. Harrowell, M. Murato, V. A. Norris, and H. C. Freeman. 1986. Crystal structure analyses of reduced (Cu^{I}) poplar plastocyanin at six pH values. *J. Mol. Biol.* 192:361–387.

Hendrickson, W. A. 1985. Stereochemically restrained refinement of macromolecular structures. *Methods Enzymol.* 115B:252–270.

Hua, X. Q., S. E. Shoelson, M. Kochoyan, and M. A. Weiss. 1991. Receptor binding redefined by a structural switch in a mutant human insulin. *Nature (Lond.).* 354:238–241.

Jones, T. A. 1978. A graphics model building and refinement system for macromolecules. *J. Appl. Crystallogr.* 11:268–272.

Kabsch, W. 1988. Evaluation of single-crystal X-ray diffraction data from a position-sensitive detector. *J. Appl. Crystallogr.* 21:916–924.

Kalata, K. 1985. A general purpose computer-configurable television area detector for x-ray diffraction applications. *Methods Enzymol.* 114:486–511.

Kalata, K., W. C. Phillips, M. Stanton, and Y. Li. 1990. Development of a synchrotron CCD-based area detector for structural biology. *Proc. Soc. Photo-opt. Instr. Eng.* 1345:270–280.

Karle, I., J. L. Flippen-Anderson, S. Agarwalla, and P. Balaram. 1991. Crystal structure of [Leu^{1}]zervamicin, a membrane ion-channel peptide: implications for gating mechanisms. *Proc. Natl. Acad. Sci. USA.* 88:5307–5311.

Nar, H., A. Messerschmidt, R. Huber, M. van de Kamp, and G. W. Ganters. 1991. Crystal structure analysis of oxidised *Pseudomonas aeruginosa* azurin at pH 5.5 and pH 9.0. *J. Mol. Biol.* 221:765–772.

Pflugrath, J. W., and A. Messerschmidt. 1987. Fast system software. *In* Computational Aspects of Protein Crystal Data Analyses: Proceedings of the Daresbury Study Weekend, 23–24 January 1987. J. R. Helliwell, P. A. Machin, and M. Z. Papiz, editors. Science and Engineering Research Council, Daresbury Laboratory, Daresbury. 149–161.

Rayment, I., J. E. Johnson, and D. Suck. 1977. A method for preventing crystal slippage in macromolecular crystallography. *J. Appl. Crystallogr.* 10:365.

Richardson, D. C., and J. S. Richardson. 1992. The kinemage: a tool for scientific communication. *Protein Sci.* 1:3–9.

Shoelson, S. E., Z.-X. Lu, L. Parlautan, C. S. Lynch, and M. A. Weiss. 1992. Mutations at the dimer, hexamer, and receptor-binding surfaces of insulin independently affect insulin-insulin and insulin-receptor interactions. *Biochemistry.* 31:1757–1767.

Smith, J. L., P. W. R. Corfield, W. A. Hendrickson, and B. W. Low. 1988. Refinement at 1.4 Å resolution of a model of erabutoxin b: treatment of ordered solvent and discrete disorder. *Acta Crystallogr.* A44:357–368.

Smith, J. L., W. A. Hendrickson, R. B. Honzatko, and S. Sheriff. 1986. Structural heterogeneity in protein crystals. *Biochemistry.* 25:5018–5027.

Swensson, L. A., L. Sjolin, G. L. Gilliland, B. C. Finzel, and A. Wlodawer. 1987. Multiple conformations of amino acid residues in ribonuclease A. *Proteins.* 1:370–375.